Numerical study of the influence of the parameters of statistical distribution of the structural elements' ultimate strength on deformable bodies' fracture processes

E.V. Feklistova, A.I. Mugatarov, V.E. Wildemann
Center of Experimental Mechanics, Perm National Research Polytechnic University, Russia
cem.feklistova@mail.ru, https://orcid.org/0000-00020025-6204
cem_mugatarov@mail.ru, https://orcid.org/0000-0002-2229-8181
wildemann@pstu.ru, https://orcid.org/0000-0002-6240-4022

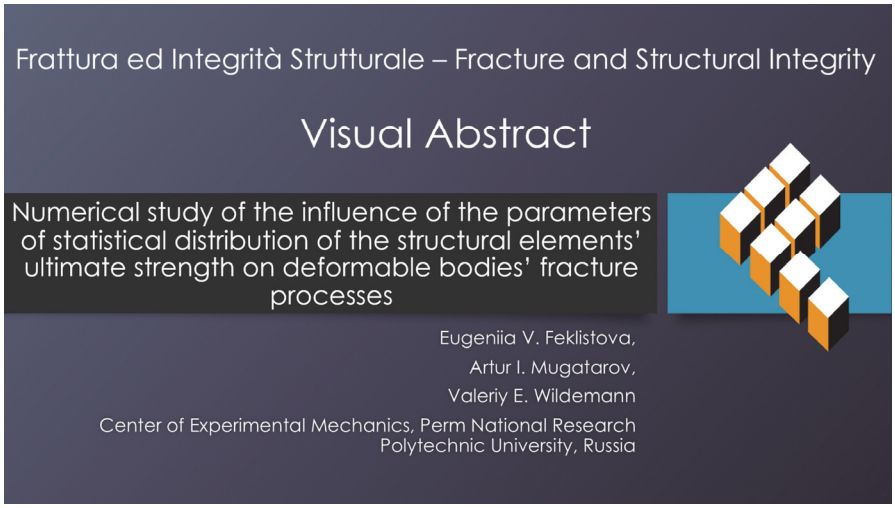

Citation: Feklisova, E.V, Mugatarov, A.I., Wildemann, V.E., Numerical study of the influence of the parameters of statistical distribution of the structural elements' ultimate strength on deformable bodies' fracture processes, Frattura ed Integrità Strutturale, 70 (2024) 105-120.

Received: 18.06.2024
Accepted: 08.08.2024
Published: 12.08.2024
Issue: 10.2024

KEYWORDS. Fracture, Finite element method, Numerical modeling, Brittle body, Strength properties distribution.

INTRODUCTION

To ensure the reliability and safety of critical structures, it is necessary to analyze their mechanical behavior not only under conditions of normal operation, but also under conditions of fracture processes at the macrolevel [1]. Various computational methods are used to analyze the processes of solid's deformation and fracture. The most widely used approaches are: finite element method [2], extended finite element method [3, 4], extended virtual element method [5], peridynamics [6], finite element discretized symplectic method [7], meshfree method [8], etc. In addition, various models of materials' mechanical behavior are used: linear elastic model [9] (in linear elastic fracture mechanics), continuum damage models [10], cohesive crack models [4], bridged crack models [11], etc. An approach, in which the change of finite elements' (FE) stiffness properties is implemented when the failure criterion is fulfilled, is widely used during numerical modeling of

fracture processes [[12]–[14]]. The advantages of this approach are: a simplicity of using, an absence of necessity in the mesh rebuilding after each act of destruction, a possibility of implementing complex stiffness reduction schemes to take into account various mechanisms of structural damage (for example, delamination [13] or fibers fracture [12, 14]). However, this approach requires consideration of several aspects.

Firstly, since the reduction of FE's stiffness after the failure criterion implementation leads to a change in the stress-strain state, the fracture process should be carried out under constant boundary conditions until a stable state is obtained. Therefore, it is necessary to recalculate the stress-strain state after each FE's deactivation by additional iterative procedures included into programs of the fracture processes numerical modeling. Researchers use various criteria to define the end of the iterative procedures. For example, Zheng et al. [12] used the criterion of the total increment exceeding the tangent constitutive tensors of fiber yarns and matrix, Yun et al. [15] considered the convergence criterion for the stress-strain state, Feklistova et al. [16, 17] applied the convergence criterion for fulfilling the strength criterion in all FEs. Secondly, the number of elements destroyed per iteration can affect the numerical results, which was demonstrated by Wildemann et al. [17]. Thirdly, the accuracy of the results of the fracture processes modeling is influenced by the size of the loading step. On the one hand, the using of a constant step value is simpler and requires less computational costs in some cases. On the other hand, the loading step value, which is automatically selected basing on the results of the boundary value problem's solution at the previous step, allows to describe the damaging process much more accurately. The effectiveness of the automatic step using in the fracture processes modeling was demonstrated by Ilinykh et al. [18, 19]. Finally, the results of the numerical modeling of the fracture process are significantly affected by the computational domain's discretization, which was shown by Prince et al. [4], Zhou et al. [20], Lopes et al. [21], and many other authors. In the boundary value problems of the elasticity theory, an increase in the number of degrees of freedom leads to an improved convergence. On the contrary, in the fracture processes modeling the FE's size reduction may significantly change the results. Prince et al. [4], Lopes et al. [21] carried out the choice of the rational FE's size by comparing the results of the numerical modeling with the experimental data. All the above aspects have been considered in paper [17]. It was demonstrated that to simulate the deformation and fracture processes of the elastic-brittle bodies, it is necessary to use the iterative procedure for recalculating the stress-strain state at the current loading step until the stable state is achieved; to deactivate only one (the most overloaded) FE per iteration; to select the loading step value automatically; to use the FE's size obtained by the comparing the experimental results with the numerical data, since this approach allows to determine the physically justified FE's size.

The results of the fracture processes modeling are also significantly affected by the inhomogeneity of the structural elements' mechanical properties distribution over the body volume [[12], 16, [22]–[24]]. Zheng et al. [12] performed the multiscale modeling of 3D woven composites assuming that the fibers' strength follows the two-parameter Weibull distribution. It was noted that the large value of the strength distribution dispersion advances the occurrence of fiber breakage, leading to an earlier damage development. Hai et al. [22] modeled the destruction of concrete, the tensile strength fields were generated using Gaussian, lognormal, Gamma, Gumbel, and Weibull distributions. It was noted that the variability of the peak force increased significantly if the correlation length was enlarged. Chen et al. [23] developed an extended two-scale random field model for the stochastic response analysis of concrete structures. Probabilistic characteristics of the compressive and tensile strength fields were generated using the lognormal distribution. The authors noted that the larger correlation length had smaller peak values and broader distribution ranges. If the spatial variability was not taken into account in stochastic response analysis, the tail of the probability distribution for the shear wall responses would be misestimated, resulting in a misleading structural reliability assessment. Liu et al. [24] studied the behavior of the concrete, represented as an assembly of parallel meso-springs. The stress-strain relationship of the meso-springs followed the elastic-brittle assumption, the material properties were assumed to be random. Consideration of the inhomogeneity of the mechanical properties' distribution is especially important in the study of the fracture processes of the bodies with the stress concentrators. In the previous study [16] the authors of the work demonstrated that the variation of the structural elements' strength properties affects the structure's macro-level behavior, the load-bearing capacity of the body, and the kinetics of damage accumulation process. Nevertheless, it is important to carry out a more detailed study of the influence of various parameters of the mechanical properties' probability distribution on the results of the fracture processes modeling. Moreover, since the numerical modeling of these processes requires high computational costs, development of the methods that qualitatively allow to predict the bodies' fracture processes basing on the results of the boundary value problem's solution within the elasticity theory, has a great promise.

In this work, a numerical study of the fracture processes of the elastic-brittle bodies with randomly distributed structural elements' strength properties is carried out. In the section "Methodology" main findings and limitations of the previous study [16] are discussed, and the methodology of this work is described. In the section "Boundary value problem and its solution algorithm" the formulation of the boundary value problem is given, the algorithm for its numerical solution is considered, and the problem of the deformation of the plate with a stress concentrator is formulated. The section "Results"

represents the fracture processes patterns obtained by the numerical modeling. The in-depth analysis of the results is provided in the section "Discussion". In the section "Conclusions" the main conclusions of the work are given and directions for further research are outlined.

METHODOLOGY

Previously, the authors in work [16] carried out the numerical study of the destruction processes of bodies with stress concentrators, taking into account the probability distribution of the strength properties of the structural elements. The following assumptions were taken:

- The material was elastic-brittle, there was no plastic deformation in the body, viscoelastic behavior and contact interaction (for example, friction) between the damaged zones.
- One FE corresponded to one subregion, within which the properties were homogeneous.
- Despite the distribution of the strength properties, the elastic characteristics were similar for all subregions.

During computational experiments, the following data was obtained:

- External load values for various values of the body's boundary displacement. Using these points, the loading diagrams were constructed and analyzed, reflecting the macro-level behavior of the solid.
- The number of the FEs deactivated per iteration of the algorithm. Based on these data, the dependences of the relative number of the deactivated elements on the body's boundary displacement were plotted.
- Number of the element being deactivated on current iteration. This data allowed to restore damaged zones in the body without maintaining the stress-strain state in all FEs. Using these results, the images of the body were obtained, reflecting the evolution of damaged zones (i.e. the process kinetics could be studied).

The main findings of previous research were:

- The fracture process consideration allows identifying the additional load bearing capacity.
- The postcritical deformation stage implements if the dispersion of the probability distribution of FEs' ultimate strength is large (characterized by the parameter α).
- The maximum load value depends nonmonotonically on α, the maximum is achieved at $\alpha=0.6$.
- The distribution range increase leads to a significant growth in the number of the deactivated FEs.
- The basic mechanisms of the damage accumulation are: the elements destruction in the stress concentration zone leading to the macro-defect growth; the elements fracture near the macro-defect; the elements destruction far from the stress concentrator.
- The concentrator's depth decrease leads to the change in the damage accumulation kinetics and the maximum load dependence on the parameter α.
- The hypothesis was put forward on existence of the critical α parameter value, upon reaching which the stress concentrator stops influencing the fracture process.

However, the previous work had some disadvantages and limitations:

- The model material with the Young's modulus E=210 GPa and Poisson's ratio ν=0.3 was considered. Despite the fact that this is a model material, the potential possibility of the experimental verification of the obtained results is of interest. In this regard, it is relevant to use in the work a model material with properties corresponding to a real material, which behaves as the elastic-brittle one.
- Only the uniform distribution was considered. Moreover, the dispersion of the mechanical properties was specified using the artificially introduced parameter α. Since it is of interest to compare the results obtained using various probability distribution laws, this parameter should be replaced with a standard one (for example, variance, standard deviation, etc.).
- The characteristic types of the damage accumulation process were mentioned. However, these types were not sufficiently disclosed and a clear connection was not made between the fracture type and the load-bearing capacity of the body.
- The areas of the application of the obtained results were not sufficiently disclosed.

While maintaining the basic assumptions and the types of the data obtained during numerical modeling, in order to correct the identified disadvantages and limitations, in this work more attention is paid to the influence of the both the probability distribution law and the dispersion of the ultimate strength properties on the fracture processes of the body with the stress concentrator. A more detailed analysis of the macro level behavior and the kinetics of the damaging process is carried out; the main types of the damage accumulation are thoroughly described. In addition, since the fracture processes modeling

requires significant computational costs, the possibility of predicting the kinetics of the fracture process based on the results of the solutions of the boundary value problems of the elasticity theory is additionally tested.

BOUNDARY VALUE PROBLEM AND ITS SOLUTION ALGORITHM

Mathematical formulation

The solid is represented as a set of N subregions, whose material is homogeneous and isotropic; the elastic properties are equal for all the subregions. In order to take into account the inhomogeneity of subregions' ultimate strength, the indicator function can be used:

$$\chi^{(m)}(\bar{r}) = \begin{cases} 1, \bar{r} \in V_m \\ 0, \bar{r} \notin V_m \end{cases}$$

$$\sigma_B(\bar{r}) = \sum_{m=1}^{N} \sigma_B^{(m)} \chi^{(m)}(\bar{r}) \tag{1}$$

Here $\bar{r}$ is the radius vector; $\chi^{(m)}$ is the indicator function, characterizing the point location in the subregion indexed (m) with the volume V_m; V is the entire body volume; σ_B is the piecewise-constant function that specifies the ultimate strength values distribution over the solid.

As the fracture process is considered, the process parameter t (a conditional analogue of time) must be introduced into the problem to take into account the history of the damaging process. Thus, any stress, strain or displacement component should depend not only on the coordinates, but the process parameter too.

Since each subregion is elastic-brittle, the assumption is made that the destruction of subregion occurs when the maximum value of the first principal stress σ_1 in the subregion's volume reaches the ultimate strength value. Nevertheless, each subregion has its own value of ultimate strength, so it is more convenient to introduce into the problem the relative parameter, indicating the failure risk in various subregions of the solid. Therefore, the overload factor K is considered:

$$K(\bar{r},t) = \frac{\sigma_1(\bar{r},t)}{\sigma_B(\bar{r})} \tag{2}$$

The value of K exceeding 1 indicates that subregion should be destructed.

The material is elastic-brittle, so the constitutive law can be represented using generalized Hooke's law, including the integrity parameter, that defines the implementation of the failure criterion in the subregions:

$$\sigma_{ij}(\bar{r},t) = \lambda(\bar{r},t) C_{ijkl} \varepsilon_{kl}(\bar{r},t)$$

$$\lambda(\bar{r},t) = \sum_{m=1}^{N} \lambda^{(m)}(t) \chi^{(m)}(\bar{r}) \tag{3}$$

$$\lambda^{(m)}(t) = \begin{cases} 0, \exists \tau \le t : \max\limits_{V_m} \left(K(\bar{r},\tau) \right) \ge 1 \\ 1, \nexists \tau \le t : \max\limits_{V_m} \left(K(\bar{r},\tau) \right) \ge 1 \end{cases}$$

Here σ_{ij} is the stress tensor; ε_{ij} is the Lagrangian strain tensor; C_{ijkl} is the elastic constants tensor; $\lambda^{(m)}$ is the integrity parameter of the subregion (m); λ is a piecewise-constant function, reflecting the integrity parameters' distribution over the solid.

To finish the boundary value problem formulation, the equations of equilibrium (no mass forces are considered) and the strain-displacement equations (since the strains in the destructed subregions can be large, the Lagrangian strain tensor is preferrable) are applied:

$$\begin{cases} \sigma_{ij,j}\left(\overline{r},t\right)=0 \\ \varepsilon_{ij}\left(\overline{r},t\right)=\dfrac{1}{2}\left(u_{i,j}\left(\overline{r},t\right)+u_{j,i}\left(\overline{r},t\right)+u_{k,i}\left(\overline{r},t\right)u_{k,j}\left(\overline{r},t\right)\right) \end{cases} \tag{4}$$

Here u_i is the displacement vector. The problem is supplemented by the displacement boundary conditions and the traction boundary conditions:

$$\begin{cases} u_i\left(\overline{r},t\right)\big|_{\Gamma_u}=u_i^0\left(\overline{r},t\right) \\ \sigma_{ij}\left(\overline{r},t\right)n_j\left(\overline{r}\right)\big|_{\Gamma_S}=S_i^0\left(\overline{r},t\right) \end{cases} \tag{5}$$

Here u_i^0 is the displacement vector applied to the boundary Γ_u; S_i^0 is the stress vector applied to the boundary Γ_S; n_j is the unit normal vector to the boundary Γ_S. The Eqns. (1)–(5) form the boundary value problem of deformation and fracture of the solid body.

Solution algorithm

The boundary value problem (1)–(5) can be solved numerically with the finite element method; each finite element (FE) represents one subregion. The solution algorithm is:

1) Designing and meshing of the body, generating of the ultimate strength values of FE, entering of the material properties;
2) Creating of the boundary conditions (Eq. (2)), u_i^0 and S_i^0 values should be small to prevent the failure criterion fulfillment at the first step;
3) Calculating of the stress-strain state;
4) Calculating of the external load value (ELV). If its value is less than the critical value (labelled as P_{crit}), the fracture modeling process ends (except for the first step);
5) Calculating of the field of the overload coefficient (K), defining of its maximum value (labelled as K_{max});
6) If $K_{max}\geq 1$, then deactivating (failure) of the most overloaded FE and going to the step 3, else going to the step 7;
7) Magnifying of the boundary conditions $1/K_{max}$ times, going to the step 3.

The flow chart of the algorithm is presented in Fig. 1. The expediency of the proposed algorithm was proved in [[16], [17]]. As the result of the boundary value problem solution, the loading diagrams and the damage accumulation kinetics data are obtained.

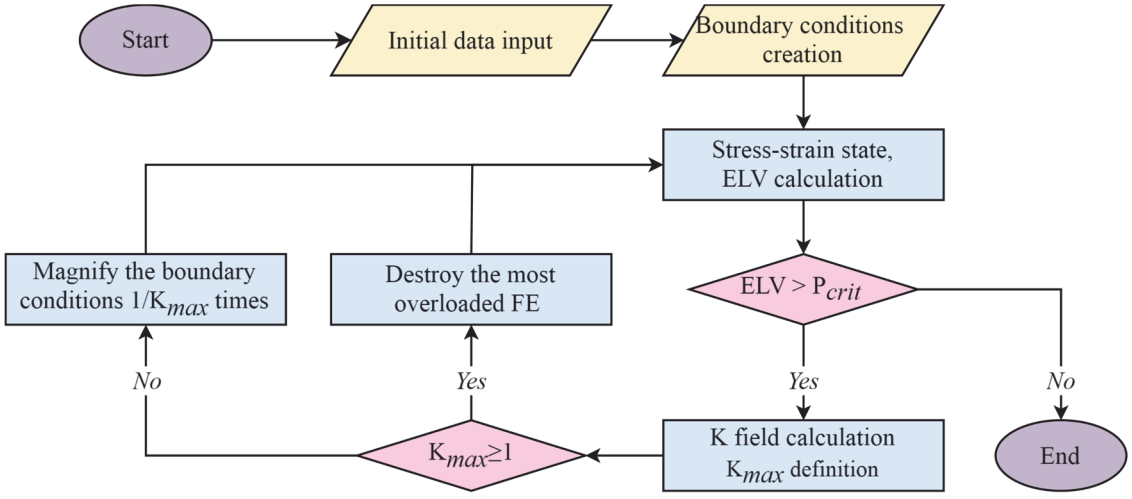

Figure 1: The flow chart of the boundary value problem solution algorithm

The abode algorithm is implemented in the Ansys Parametric Design Language (APDL). The FE's deactivating is carried out using the ANSYS built-in procedure "death of finite element", leading to the rigidity properties decrease by 10^6 times.

Model setup

In order to investigate the influence of the parameters of the statistical distribution of the strength properties on the elastic-brittle bodies fracture processes, the problem of kinematic static loading of a plate (100 mm wide, 20 mm height and 1 mm thick, plane stress state) with the stress concentrator in the shape of the half ellipse (minor semiaxis 1 mm and major semiaxis 4 mm) is considered. The body's geometry is shown in the Fig. 2.

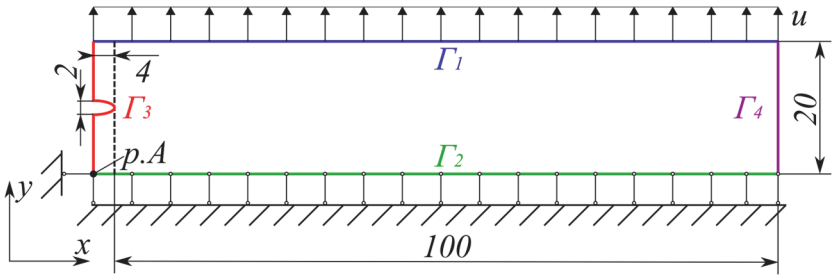

Figure 2: The geometry of the solid with the stress concentrator and the boundary conditions.

The boundary conditions are:

$$\begin{cases} u_y(t)\big|_{\Gamma_1} = u_0(t) \\ u_y(t)\big|_{\Gamma_2} = 0 \\ u_x(t)\big|_{p.A} = 0 \\ \sigma_{ij}(\bar{r},t)n_j(\bar{r})\big|_{\Gamma_3} = 0 \\ \sigma_{ij}(\bar{r},t)n_j(\bar{r})\big|_{\Gamma_4} = 0 \end{cases} \tag{6}$$

Here Γ_1, Γ_2 are the top and bottom boundaries of the body; Γ_3, Γ_4 are the left and right boundaries of the body, point A ($p.A$) is the lower left corner of the body, u_0 is the displacement of the top boundary (Fig. 2).

In order to investigate the patterns of the fracture processes of the elastic-brittle bodies taking into account the FEs strength values distribution, a model material with Young's modulus E=3 GPa and Poisson's ratio ν=0.36 (these properties correspond to the properties of the acrylic glass [25]) is considered. The ultimate strength values of finite elements were distributed using uniform distribution and 2-parameter Weibull distribution, in all the generations mean value σ_{Bm} was equal to 40 MPa. To characterize the variance of the FEs ultimate strength distribution, the parameter σ is introduced, defined as the ratio between the distribution's standard deviation and σ_{Bm} (i.e., the parameter σ is the relative value of the standard deviation). The maximum value of σ, that do not lead to the occurrence of negative values of the ultimate strength, is $\sigma_{lim}\approx0.577$. Thereby, in this investigation the values of parameter σ varied in the range from 0.0 to $0.9\cdot\sigma_{lim}$ with the step size equal to $0.1\cdot\sigma_{lim}$ (i.e., in the range from 0.0 to 0.520). The parameters of the uniform distribution and the Weibull distribution were calculated numerically to correspond chosen values of σ_{Bm} and σ. The examples of cumulative distribution functions for various values of σ are shown in Fig. 3. For each value of σ, five various sets of FEs ultimate strength values were generated.

In order to discretize the body, the PLANE182 element with the linear displacements field approximation is used, the mesh is generated automatically in ANSYS. Solving the convergence problem demonstrated that it is sufficient to use the FE with the characteristic linear size of L_{el} =0.164 mm (defined as the square root of the ratio of the body area to the number of FEs), which corresponds to the number of elements N=77104. The critical value of external load P_{crit} is selected equal to 0.1 kN to prevent the extreme increase in the displacement u_0 if the σ value is large. For a more detailed damaging process consideration, the parameter ω is introduced, defining the relative number of deactivated elements as follows:

$$\omega = \frac{N_{deact}}{N} \tag{7}$$

where N_{deact} is the number of deactivated FEs.

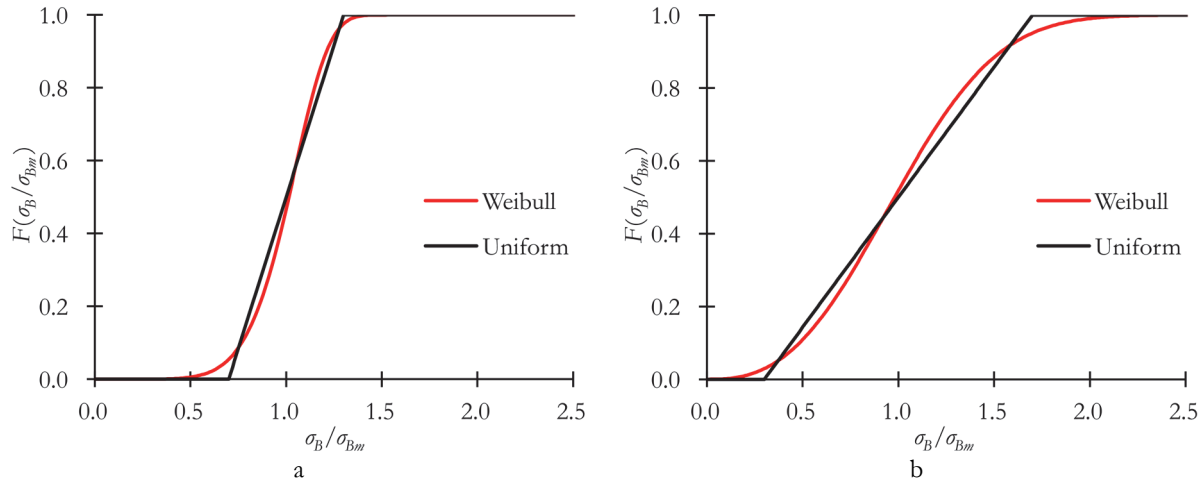

Figure 3: The cumulative distribution functions for the uniform distribution and for the 2-parameter Weibull distribution, σ=0.173 (a) and σ=0.404 (b).

Numerical experiments were carried out using the high-performance computing complex of the Center for Collective Use "Center of High-Performance Computing Systems" of the Perm National Research Polytechnic University. The results of the fracture process modeling are presented below.

RESULTS

For a better representation of the obtained results, this section is divided into subsections "Influence of the parameters of the strength properties' distribution on the loading diagrams and load bearing capacity", "Influence of the parameters of the strength properties' distribution on the kinetics of the damaging process", and "Approach for predicting the kinetics of the fracture process based on the analysis of the boundary value problem's solution within the elasticity theory".

Influence of the parameters of the strength properties' distribution on the loading diagrams and load bearing capacity

Fig. 4 shows typical loading diagrams, obtained during fracture processes' modeling by using the uniform law and the Weibull law of structural elements' strength distribution, as well as the corresponding diagrams of growth of the deactivated elements' relative number. Since the high values of the dispersion of ultimate strength distribution with the use of the Weibull distribution law has led to a significant increase in the number of required iterations and in the computational costs, the range of values of the parameter σ has been reduced to the maximum value of 0.404. The vertical sections of the loading drop correspond to an unstable fracture process, while the ascending sections correspond to the stable states in which the finite elements' fracture does not occur. The results demonstrate that with the growth of the standard deviation's value a non-monotonic change in the maximum load withstood by the body occurs. The loading diagrams gradually become smoother (especially at values σ>0.46 for the uniform distribution and σ>0.28 for the Weibull distribution), nonlinear behavior is realized at the macro level, and at σ=0.520 the realization of an extended postcritical stage of body deformation is observed [1]. The growth of σ leads to the realization of a larger number of stable states, observed as the number of deactivated elements increases, which is confirmed by the increase in the number of vertical sections on the graphs of growth of the deactivated FEs' relative number, which also gradually become smoother. Significant differences between the results obtained using various distribution laws are also discovered in the plots of the deactivated FEs' relative number. While they have a pronounced linear section at σ>0.46 at the uniform distribution, then, with the use of the Weibull distribution law, the growth of the parameter ω is non-linear and begins to appear at small values of the standard deviation

of the FEs' ultimate strength distribution. The discovered differences are explained by the presence of FEs with small values of ultimate strength at any values of dispersion in the case of using the Weibull distribution law. A more stable fracture process and the realization of a greater number of stable states are also observed.

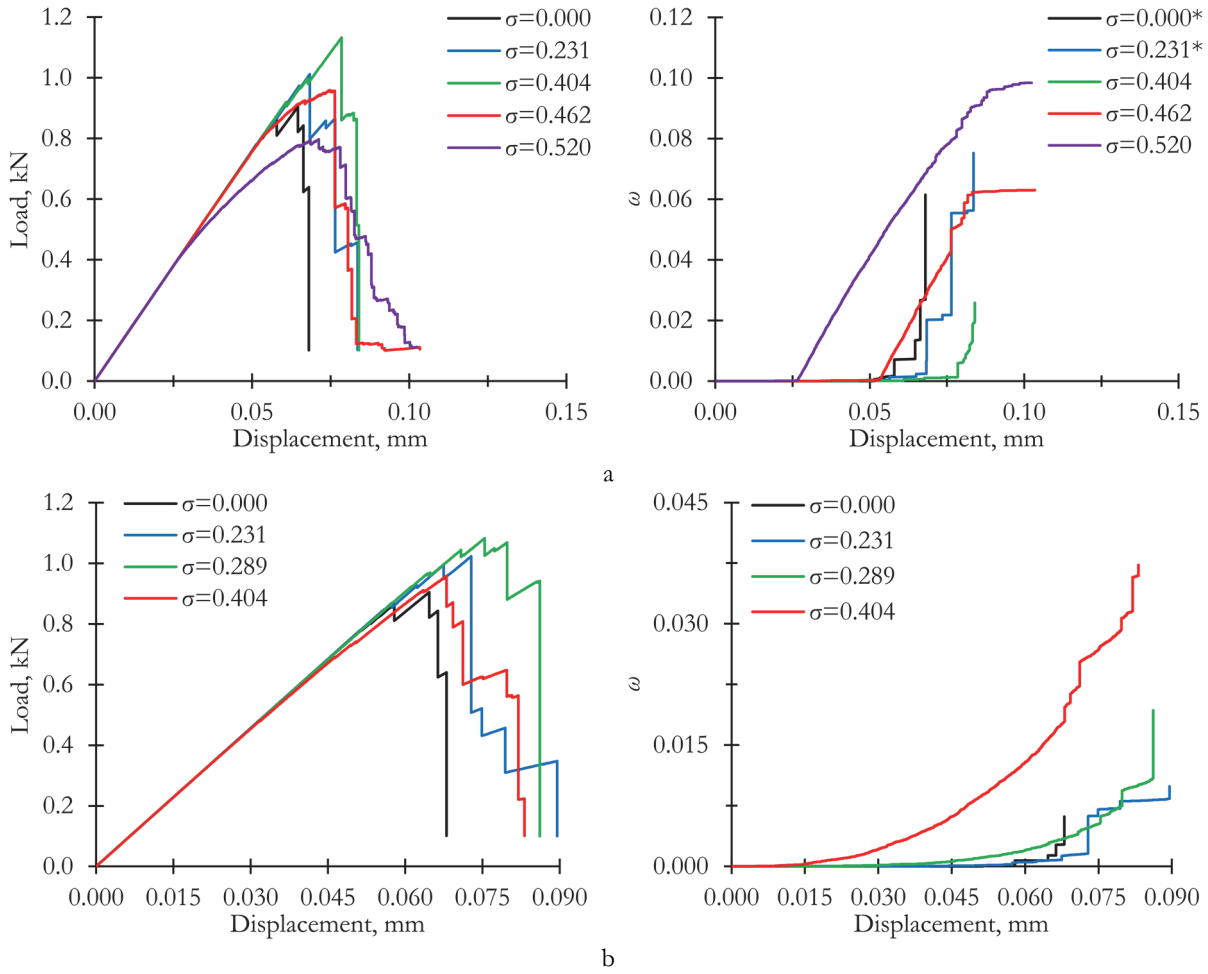

Figure 4: The calculated loading diagrams (left side) and the corresponding diagrams of growth of the deactivated elements' relative number (right side) for the various values of σ: uniform distribution (a); Weibull distribution (b). The diagram labelling with "*" means that the ω value is multiplied by 10 for better visibility.

The influence of the standard deviation value on the maximum load withstood by the body and the maximum value of the deactivated elements' relative number has been studied in detail. The obtained dependencies are shown in Fig. 5, with the dashed line connecting the mean values of the parameters for five realizations and with the standard deviations indicated by the segments. The results show that for both distribution laws with the growth of the parameter σ in the range from 0.0 to 0.24, there is a gradual increase in the load-bearing capacity of the body with the concentrator. For the uniform distribution, at the values of the parameter σ in the range from 0.28 to 0.41 the bearing capacity of the body reaches its maximum. For the Weibull distribution, a shift of the maximum point of the body's bearing capacity to the left (σ=0.289) is observed. Further increase in the parameter σ led to a significant drop in the maximum load withstood by the body, moreover, the standard deviation of this value decreased significantly. The number of deactivated elements changes only slightly at σ<0.18 for both distribution laws. However, with further growth of σ, a significant increase (exceeding 10% at σ=0.520 for the uniform distribution) in the number of deactivated FEs is observed. It is of interest to explain these effects in terms of the fracture process kinetics.

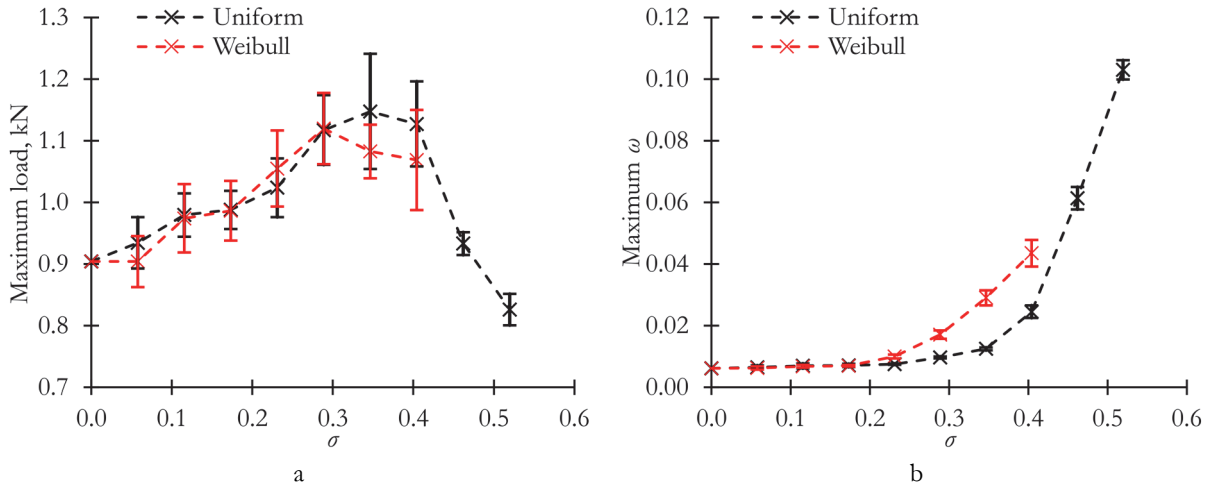

Figure 5: The dependencies of the maximum load value (a) and the maximum ω value (b) on σ.

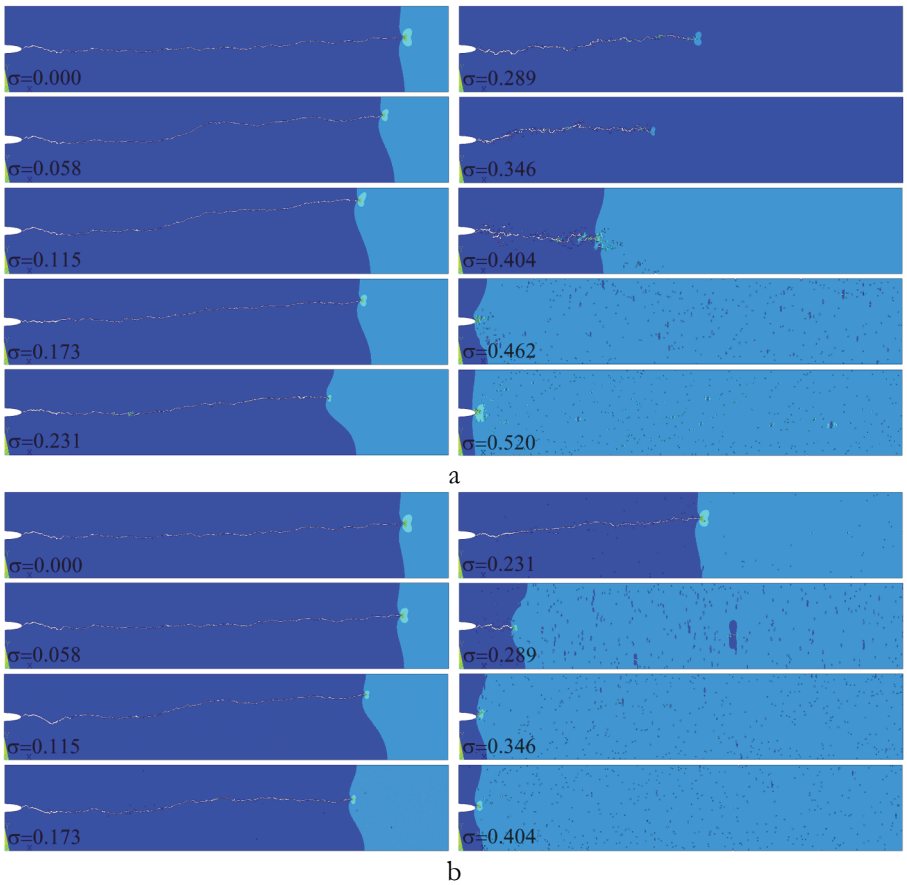

Figure 6: The images of the body with various σ at ω=0.006: uniform distribution (a); Weibull distribution (b)

Influence of the parameters of the strength properties' distribution on the kinetics of the damaging process

To determine the possible types of damage accumulation in the body, the fracture processes kinetics for the different values of the standard deviation of the finite elements' strength distribution has been analyzed. Fig. 6 shows images of the body (with the field of the first principal stress) for different values of σ at equal ω values of 0.006. The results show that at $\sigma \leq 0.24$ for the uniform distribution and $\sigma \leq 0.12$ for the Weibull distribution the macrodefect is formed as a crack with thickness of 1-2 FEs. At $0.28 \leq \sigma \leq 0.41$ for the uniform distribution and $0.17 < \sigma < 0.29$ for the Weibull distribution, which corresponds to the maximum load-bearing capacity, individual deactivated FEs are observed, located close to the microdefect, but not being

part of it. This peculiarity is explained by the presence of FEs with a small value of ultimate strength (hereinafter we will refer to them as 'weak' FEs) in the area of stress concentration. With further increase of dispersion of the FEs' ultimate strength (σ>0.46 for the uniform distribution and σ>0.34 for the Weibull distribution law), the processes of damage accumulation in the structure occur throughout the whole volume of the body, including the area far from the stress concentrator, and groups of defects with a small number of deactivated FEs are formed. This pattern can be explained by the presence of 'weak' FEs with extremely low ultimate strength.

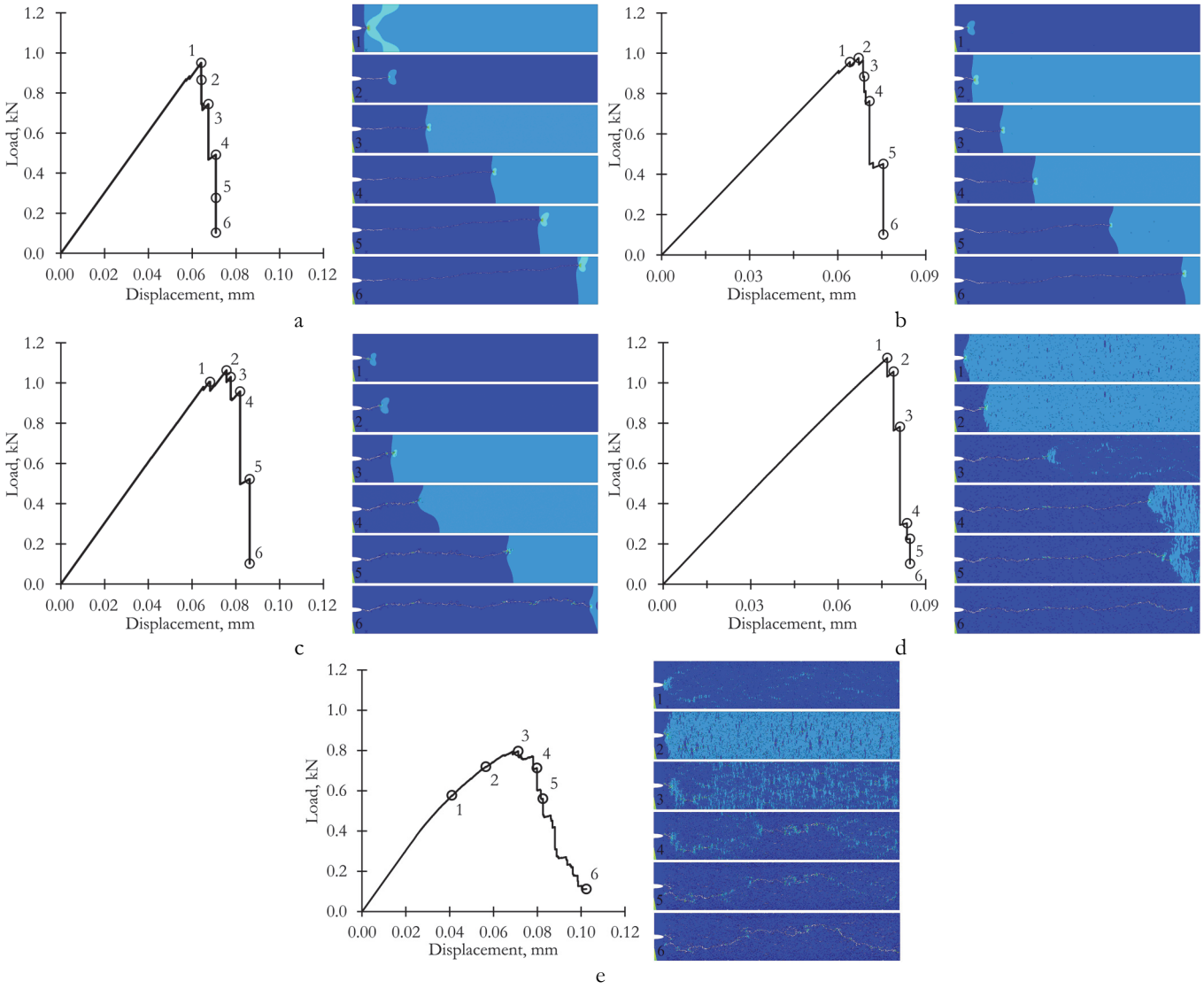

Figure 7: The calculated loading diagram (left side) and the evolution of damaged zones (right side): uniform distribution, σ=0.173 (a), Weibull distribution, σ=0.173 (b), uniform distribution, σ=0.346 (c), Weibull distribution, σ=0.346 (d), uniform distribution, σ=0.520 (e)

For a deeper understanding of the fracture process kinetics, the evolution of damaged zones in the body has been additionally analyzed. Fig. 7 shows some loading diagrams and images of the body (with the fields of the first principal stress), corresponding to the states indicated in the loading diagrams. At σ=0.173, almost no damage accumulation occurs until the maximum load is reached for both distribution laws, the macrodefect grows from the initial stress concentrator, the fracture of each next FE occurs at the tip of the propagated crack. The presence of stable states is explained, on the one hand, by the peculiarities of the mesh generation, on the other hand, by the presence of FE with a high value of ultimate strength (hereinafter we will refer to them as 'strong' FEs) on the crack propagation path, as for the fracture of strong FE the external load must be increased. At σ=0.346, sufficiently developed fractures are observed even before the maximum load is reached. The increase in the dispersion of the distribution of the structural elements' strength properties led to the appearance of 'weak' FEs in the area of stress concentration near the crack tip, which promotes fracturing of FE, located

near the macrodefect, but separated from it. However, the using of the Weibull distribution led to the fracture of several FEs in the body's volume, far from the microdefect. This pattern is explained by the appearance of many FEs with extremely low values of the ultimate strength. At σ=0.520, predominantly dispersed accumulation of structural damage is observed both near the stress concentrator and in the body volume. Consequently, the growth of dispersion of the structural elements' strength properties leads to weakening of stress concentrator influence. The maximum load in the body is reached when the structure is significantly damaged, with the higher number of FEs fractured before the maximum load is reached than afterwards. A macrodefect, which leads to the loss of the load-bearing capacity, propagates by combining small damaged regions.

Approach for predicting the kinetics of the fracture process based on the analysis of the boundary value problem's solution within the elasticity theory

In order to predict the fracture process kinetics, it is of interest to study the material state in the zone with increased stresses occurring near the concentrator. For the considered body this zone was selected in the following way: the first principal stress field σ_1 was calculated from the results of the boundary value problem solution within the elasticity theory, and the value of this stress was determined in the finite element, the most distant from the concentrator, lying on the symmetry axis of the body (the obtained value is denoted as σ_{1far}). After that, the finite elements with σ_1 values exceeding σ_{1far} by more than 3.5% were selected (thus, a single region of increased stresses was obtained instead of a set of several regions). A detailed analysis of the obtained stress concentration zones will be given below.

For a small displacement of the body's boundary, solutions of boundary value problems within the elasticity theory are obtained for those sets of finite elements' ultimate strength values that were previously used in the fracture processes modeling. Calculation of the fields of overload coefficients K by Eqn. (2) has been carried out. Examples of the overload coefficient fields for different values of the standard deviation of the finite elements' ultimate strength are shown in Fig. 8 (left side). It should be noted that two factors influence the type of the resulting fields: the distribution of finite elements' ultimate strength and the inhomogeneity of the stress field due to the presence of the concentrator. The results show that as the value of the parameter σ increases, the dispersion of the overload coefficients distribution increases. In addition, when σ grows to 0.404, an increase in the maximum value of K is observed, which is explained by the presence of 'weak' elements in the stress concentration zone. Those FEs will be referred to overloaded, in which the value of K exceeds 50% of the maximum overload coefficient value in the body (K_{max}), and those FE's will be refereed to underloaded, in which the value of K is less than 15% of K_{max}. Fig. 8 (right side) shows images, reflecting the distribution of overloaded and underloaded FEs (marked in red and blue, respectively) in the stress concentration zone. On the basis of the analysis of these images, a number of patterns are identified. Firstly, at σ<0.24 for the uniform distribution and at σ<0.12 for the Weibull distribution, the number of overloaded FEs in the stress concentration zone almost does not change. Meanwhile, at σ=0.289 a sharp jump in this number is observed for the uniform distribution. On the one hand, this phenomenon can be explained by the absence of FEs in the concentrator at low values of σ, when FEs have such a high ultimate strength that the overload coefficient is small even under condition of stress concentration. On the other hand, at higher value of σ, the occurrence of FEs with low values of ultimate strength takes place, as FEs ensure high values of overload coefficients. Secondly, the growth of the standard deviation of the FEs strength values distribution leads to an almost monotonic increase in the number of underloaded elements, which is explained by the appearance of FEs with increased strength values, and by an increase in the maximum value of the overload coefficient. Moreover, for the Weibull distribution, no overloaded FEs are observed in the stress concentration zone. Thirdly, at σ<0.24 for the uniform distribution and at σ<0.12 for the Weibull distribution, the overloaded elements are concentrated in a small region near the stress concentrator, while at higher values of σ there is a gradual dispersion of such FEs over the body volume. This is explained by the appearance of FEs with such low values of the ultimate strength that they can become overloaded even outside the stress concentration zone. At the same time, elements, with such high ultimate strength that the value of the overload coefficient will be small, may appear near the stress concentrator.

It is of interest to introduce quantitative parameters, reflecting the identified patterns. For this purpose, firstly, the number of overloaded FEs in the whole volume of the body (we denote this value as η) should be considered. Secondly, to reflect the degree of overloaded FEs dispersion over the body's volume, the value of the average distance from the tip of the stress concentrator to the centers of these FEs in the whole volume of the body (we denote this value as λ) should be taken into consideration. The dependencies of the parameters λ and η, as well as their standard deviations σ_λ and σ_η (calculated from five generations of the FE ultimate strengths), on the value of the parameter σ are shown in Fig. 9 (the values for σ=0.520 are not shown in the figures because they are extremely high, as well as their values of standard deviations). The results demonstrate that for the both distribution laws the constructed dependencies are non-monotonic, and their type at σ<0.41 qualitatively corresponds to the dependence of the maximum bearing capacity on σ (Fig. 5).

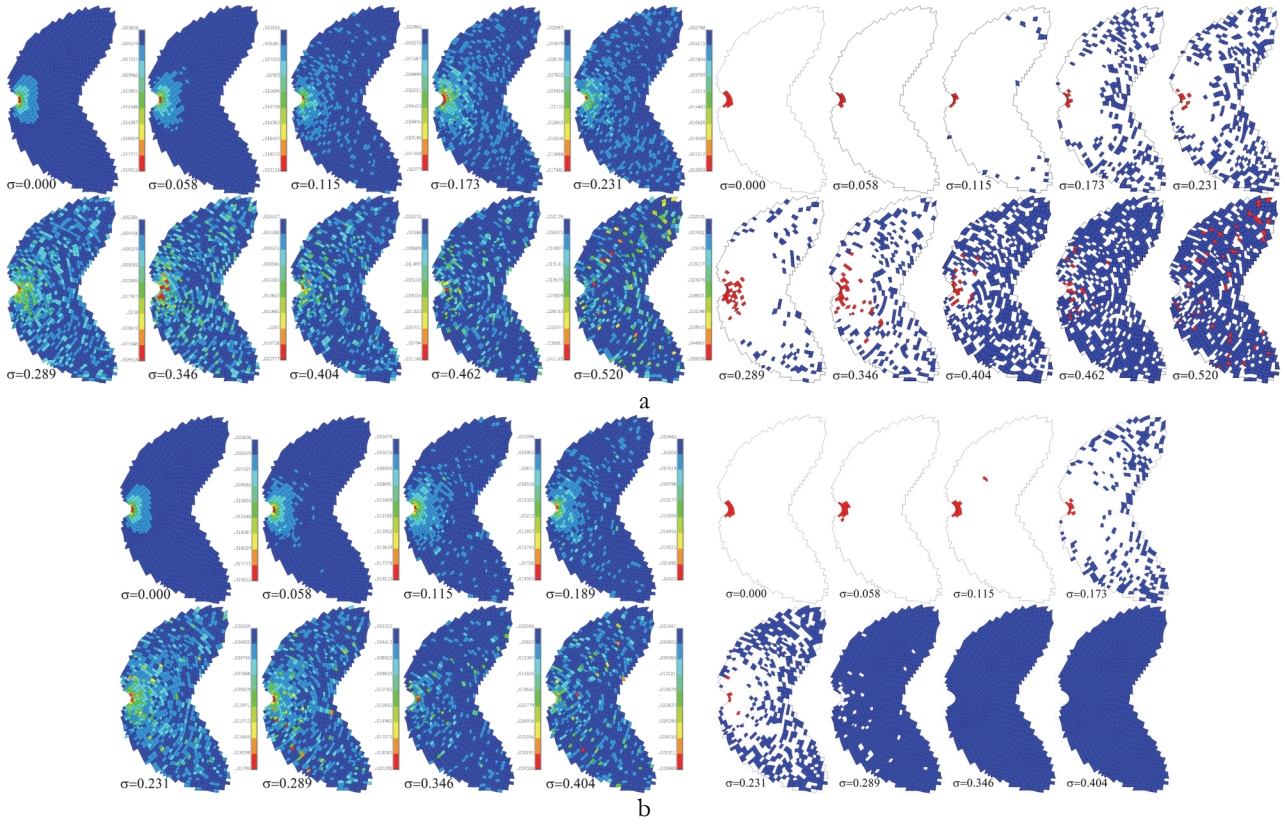

Figure 8: The overload coefficient fields in the stress concentration zone (left side) and images, reflecting the distribution of overloaded (marked as red) and underloaded (marked as blue) FEs (right side) for the various values of σ: uniform distribution (a), Weibull distribution (b)

For the uniform distribution, at σ<0.24 the values of the parameters λ and η change slightly, their standard deviations are low. This range corresponds to the macrodefect growth in the form of a single crack and to the increase in the load bearing capacity, which is explained by the occurrence of the 'strong' FEs on the crack path. The first significant increase in the values of the parameters λ and η and their standard deviations occurs when σ=0.289 is reached, which corresponds to the range where the body has its maximum bearing capacity and multiple FEs' deactivation occurs in the stress concentration zone during the damaging process. When σ=0.462 is reached, there is an increase in the average distance from the tip of the concentrator to the most overloaded elements, while their number begins to decrease, which is explained by the occurrence of the 'weak' FEs with very low ultimate strength value. This range also corresponds to the drop in the bearing capacity of the body.

For the Weibull distribution, at σ<0.12 the value of the parameter λ is low, its value is comparable to the value, obtained by using the uniform distribution law. The number of the overloaded elements η is also low, and with an increase of σ, there is only a small growth in the standard deviation σ_η, associated with an increase in the probability of 'weak' FEs occurrence. After reaching the value σ=0.173, a sharp increase in the values of the parameters λ and η, as well as their standard deviations σ_λ and σ_η, is observed, which is explained by the appearance of the FEs with a very low ultimate strength value and a high overload coefficient for some generations. Increase in the value of the parameter σ in the range from 0.17 to 0.29 leads to growth in the average distance to overloaded FEs and to a decrease in the number of overloaded Fes. In this range, multiple FEs' deactivation occurs in the stress concentration zone during the damaging process. It should be noted that the maximum load-bearing capacity of the body is achieved in this range, at high values of λ, but at low values of the parameter η, corresponding to the values, obtained at small dispersions of the strength properties distribution. The FEs deactivation in the body volume far from the stress concentrator begins to appear at σ>0.34, in this range the minimum of the function $\eta(\sigma)$ and the maximum of the function $\lambda(\sigma)$ are reached, which is associated with a high probability of FEs occurrence with a very low value of the ultimate strength in an arbitrary point of the body.

It follows from the above that the change in the kinetics of the damage accumulation process can indeed be predicted on the basis of analyzing the dependencies $\lambda(\sigma)$ and $\eta(\sigma)$ obtained from the solutions of boundary value problems within the

elasticity theory. In addition, it should be noted that for the correct identification of the damage accumulation kinetics it is desirable to use the dependencies $\lambda(\sigma)$ and $\eta(\sigma)$ not separately, but together, in order to obtain the most reliable prediction.

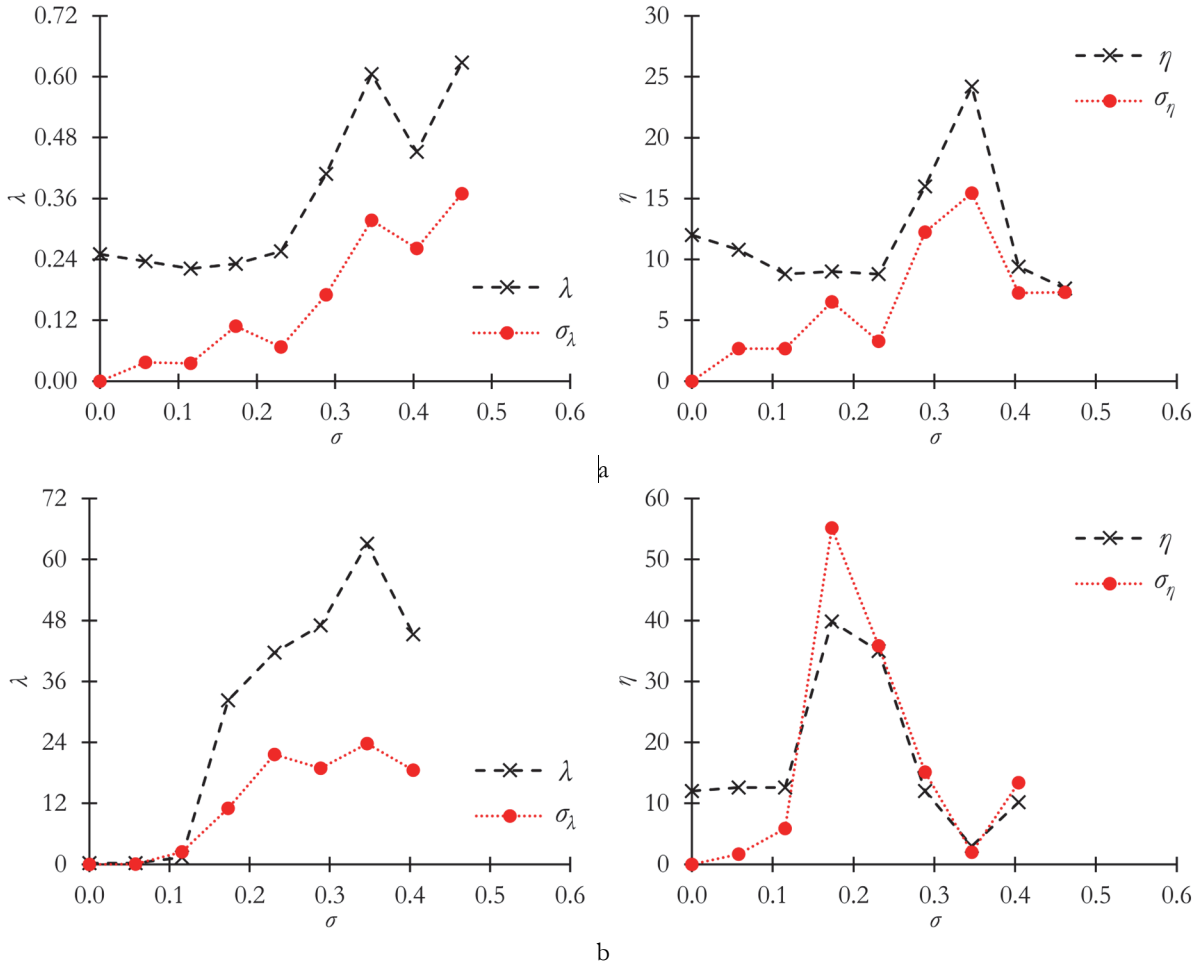

Figure 9: The dependencies of the average distance from the tip of the stress concentrator to the centers of overloaded FEs λ (left side) and the number of overloaded FEs η (right side) on σ: uniform distribution (a), Weibull distribution (b)

Discussion

Based on the results, it can be concluded that the change in the parameters of the probability distribution of the FEs' ultimate strength values significantly influences the fracture process of the body with the stress concentrator. However, the distribution law does not qualitatively change the macrolevel behavior and the damaging process kinetics. It is noted that the usage of 2-parameter Weibull distribution leads to the occurrence of the FEs with the extremely low value of the ultimate strength. On the one hand, it can be used to model pores in the structure of the material and to study their influence on the fracture process. On the other hand, it may significantly affect the results, especially the damaging process kinetics. Thus, the usage of 3-parameter Weibull distribution might be more appropriate.

The analysis of the fracture process kinetics demonstrates that for an elastic-brittle body three types of damage accumulation process are characteristic (schematically presented in Fig. 10), depending on the standard deviation of the distribution of the structural elements' strength properties. Firstly, it is a localized type of damage accumulation with macrodefect growth during FE's fracture at the tip of the propagated crack. This type is characterized by a small number of stable states and a small number of deactivated FEs before the maximum load is reached. Localized damage accumulation occurs at $\sigma<0.24$ for the uniform distribution and at $\sigma<0.12$ for the Weibull distribution. The growth of the body's bearing capacity with increasing σ in this range is explained by the appearance of 'strong' FEs on the path of macrodefect growth and the need to increase the external load to fracture them. Secondly, it is a dispersed damage accumulation in the whole volume of the body. This type is characterized by the implementation of pseudo-ductile behavior at the macrolevel, by a significant number

of stable states and a large number of deactivated FEs before the maximum load is reached. Dispersed damage accumulation occurs at σ>0.46 for the uniform distribution and at σ>0.34 for the Weibull distribution. Low load-bearing capacity is associated with an increase in the proportion of deactivated FEs in the cross-section of the body due to the developed damaged structure. Thirdly, it is a mixed type, in which the most 'weak' FEs are firstly destroyed in the area of stress concentration at the tip of the macrodefect, then the macrodefect develops by sprouting through the resulting local weakened area. In this case, the first type is hindered by the presence of 'strong' FEs on the macrodefect growth path, and the second type is hindered by the absence of 'weak' FEs in the body volume. This type is characterized by the gradual development of a macrodefect from the initial stress concentrator and by the average number of stable states. The mixed type of damaging process occurs at $0.28<\sigma<0.41$ for the uniform distribution and at $0.17<\sigma<0.29$ for the Weibull distribution. The maximum load-bearing capacity of the body is realized exactly in this range of σ values, as it is required to achieve a high external load sufficient to form a weakened local area that will not prevent further propagation of the macrodefect.

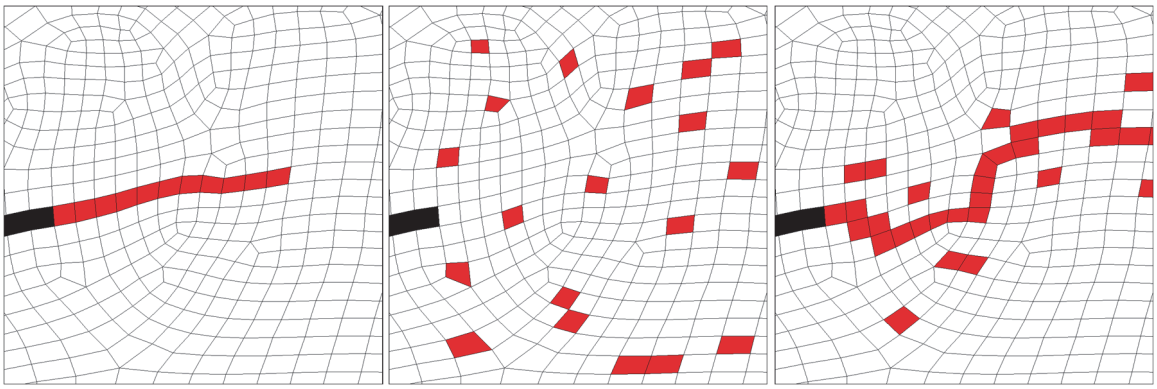

Figure 10: Characteristic types of damage accumulation: localized type (a); dispersed damage accumulation (b); mixed type (c) (black color illustrates initial macrodefect; red color illustrates deactivated FEs)

Thus, the study has allowed to reveal characteristic types of the damaging process kinetics of the elastic-brittle body with the stress concentrator. Moreover, these types reflect the macrolevel behavior of the solid and its load bearing capacity. Nevertheless, it should be noted that the ranges of the parameter σ, corresponding to the realization of the indicated types of the damage accumulation process, depend on the strength properties' distribution law and may depend on the FE's size, the body discretization method, and the geometry of the stress concentrator. Therefore, further research should be provided in order to clarify these dependencies.

The modeling of the fracture processes takes significant computational costs, especially if the dispersion of the FEs' strength properties is high. So, the approach for prediction of the fracture processes kinetics based on the results of boundary value problems' solutions within the elasticity theory has been proposed. The introduced parameters λ and η and their dependencies on the parameter σ allow to determine the realization of different types of damage accumulation without direct modeling of fracture processes, which extremely reduces the computational costs. The identified damaging process kinetics may allow to define the conditions of the realization of the maximum load bearing capacity. It is worth noting that the described approach requires a detailed analysis of many methodological aspects. In particular, it is the determination of threshold values of overload coefficients, by which overloaded and underloaded finite elements can be determined. The disadvantage of this approach is that the analysis of the results must take into account the distribution law. In this work, only five sets of FEs' ultimate strength were used to obtain dependencies $\lambda(\sigma)$ and $\eta(\sigma)$, so further modeling should be carried out to clarify the results. Nevertheless, the applicability of this approach to predict the damaging process kinetics for the solids with other stress concentrator geometries and FEs' sizes seems to be practical.

Thus, following the methodology developed by Feklistova et al. [16], this study has expanded the understanding of the damaging process kinetics. The disadvantages of the previous work, connected with the usage of the model material without any possibility of the experimental verification of the results, have been taken into account. The experimental investigation of the fracture processes of the specimens made of acrylic glass is planned to verify the results obtained in this study. Moreover, this investigation will help to create the numerical and experimental methods to define the material parameters (such as a characteristic damage zone size and a characteristic variance of the structural elements' strength properties) reflecting the fracture behavior. Proposed methodology can be successfully applied to describe the patterns of the fracture processes of the structures made of materials in which the probability distribution of the mechanical properties of the

structural elements takes place, for example, rocks, ceramics, additively manufactured metallic materials, fiber reinforced polymer composites, etc.

Conclusions

In this paper the influence of the parameters of probability distribution of the structural elements' ultimate strength on the fracture processes of the deformable bodies has been studied. The main results of the study are:

- The influence of the standard deviation of the ultimate strength distribution on the type of loading diagrams of a body with a stress concentrator has been considered in detail. The non-monotonicity of the dependence of the body's bearing capacity on the value of the dispersion of the ultimate strength distribution has been found. The fracture process kinetics has been investigated, and three types of damage accumulation has been found: localized, dispersed and mixed.
- The influence of the ultimate strength distribution law on the macro-level behavior of the body, as well as on the fracture process kinetics, has been studied. It is noted that the change in the distribution law does not lead to a change in the types of damage accumulation, but causes a change in the σ ranges, in which these types are realized.
- An approach, allowing to predict the realizable type of damage accumulation based on the results of analysis of boundary value problems' numerical solutions within the elasticity theory, has been developed. It has been proposed to consider inhomogeneous fields of overload coefficients with the calculation of two parameters: the average distance from the tip of the stress concentrator to the overloaded finite elements and the number of these finite elements. The analysis of non-monotonic dependencies of these parameters on the value of the standard deviation of the FEs ultimate strength distribution makes it possible to establish the type of damage accumulation. The feasibility of the developed approach has been demonstrated.

Further research will be directed to the detailed analysis of the influence of body's geometry and finite elements' mesh size on the fracture processes of the bodies with stress concentrators, as well as to the study of the applicability of the developed approach for predicting the fracture process kinetics.

Acknowledgements

This research was funded by Ministry of science and higher education of the Russian Federation (Project № FSNM-2024-0013).

References

[1] Sokolkin, Yu., Vil'deman, V. (1993). Post-critical deformation and failure of composite materials. Mech. Compos. Mater., 29, pp. 120–126. DOI: 10.1007/BF00696441.

[2] Zhang, X.-Q., Zhang, X., Li, L., Duan, S.-W., Li, S.-Z., Huang, Z.-L., Zhang Y.-W. and Feng, J.-Y. (2016). Investigation of the Influence of Small Hole on the Fatigue Crack Growth Path, J. Fail. Anal. Prev., 16, pp. 391–399. DOI: 10.1007/s11668-016-0098-x.

[3] Siguerdjidjene, H., Houari, A., Madani, K., Amroune, S., Mokhtari, M., Mohamad, B., Ahmed, C., Merah, A. and Campilho, R. (2024). Predicting Damage in Notched Functionally Graded Materials Plates through extended Finite Element Method based on computational simulations. Frattura Ed Integrità Strutturale, 18(70), pp. 1–23. DOI: 10.3221/IGF-ESIS.70.01

[4] Prince, M.B. and Sen., D. (2024). A numerical study on predicting bond-slip relationship of reinforced concrete using surface based cohesive behavior, Frattura ed Integrita Strutturale, 69, pp. 154–180. DOI: 10.3221/IGF-ESIS.69.12.

[5] Benvenutia, E., Chiozzia, A., Manzinib, G. and Sukumarc, N. (2021). Extended virtual element method for the Laplace problem with singularities and discontinuities, Comput. Methods Appl. Mech. Eng., 356, pp. 571–597. DOI: 10.1016/j.cma.2019.07.028.

[6] Ongaro, G., Bertani, R., Galvanetto, U., Pontefisso, A. and Zaccariotto, M. (2022). A multiscale peridynamic framework for modeling mechanical properties of polymer-based nanocomposites, Eng. Fract. Mech., 274, 108751. DOI: 10.1016/j.engfracmech.2022.108751.

[7] Xu, W., Tong, Z., Rong, D., Leung, A.Y.T., Xu, X. and Zhou, Z. (2017). Determination of stress intensity factors for finite cracked bimaterial plates in bending, Arch. Appl. Mech., 87, pp. 1151–1163. DOI:10.1007/s00419-017-1239-8.
[8] Rabczuk, T., Bordas, S. and Zi, G. (2010). On three-dimensional modeling of crack growth using partition of unity methods, Comput. Struct., 88(23–24), pp. 1391–1411. DOI:10.1016/j.compstruc.2008.08.010.
[9] Markides, C. and Kourkoulis, S.K. (2023). Revisiting classical concepts of Linear Elastic Fracture Mechanics-Part I: The closing 'mathematical' crack in an infinite plate and the respective Stress Intensity Factors, Frattura ed Integrita Strutturale, 17(66), pp. 233–260. DOI: 10.3221/IGF-ESIS.66.15.
[10] Kumchol, Y., Zhenqing, W., Mengzhou, C., Jingbiao, L., Tae-Jong, K., Namjin, S., Kyongsu, J. and Sakaya, R. (2019). A computational methodology for simulating quasi-brittle fracture problems, Comput. Struct., 215, pp. 65–79. DOI: 10.1016/j.compstruc.2019.02.003.
[11] Carpinteri, A. and Accornero, F. (2019). The Bridged Crack Model with multiple fibers: Local instabilities, scale effects, plastic shake-down, and hysteresis, Theor. Appl. Fract. Mech., 104, No. 102351. DOI: 10.1016/j.tafmec.2019.102351.
[12] Zheng, T., Guo, L., Ding, J. and Li, Z. (2022). An innovative micromechanics-based multiscale damage model of 3D woven composites incorporating probabilistic fiber strength distribution, Compos. Struct., 287, No. 115345. DOI: 10.1016/j.compstruct.2022.115345.
[13] Dezfuli, F.H. and Alam, M.S. (2014). Sensitivity analysis of carbon fiber reinforced elastomeric isolators based on experimental tests and finite element simulations, Bull. Earthq. Eng, 12, pp. 1025–1043. DOI:10.1007/s10518-013-9556-y.
[14] Nicoletto, G. and Riva, E. (2004). Failure mechanisms in twill-weave laminates: FEM predictions vs. experiments, Compos. Part A Appl. Sci. Manuf., 35(7–8), pp. 787–795. DOI: 10.1016/j.compositesa.2004.01.007.
[15] Yun, K., Wang, Z., He, L. and Liu, J. (2018). A damage model based on the introduction of a crack direction parameter for FRP composites under quasi-static load, Compos. Struct., 184, pp. 388–399, DOI: 10.1016/j.compstruct.2017.09.099.
[16] Feklistova, E., Mugatarov, A., Wildemann, V. and Agishev, A. (2024). Fracture processes numerical modeling of elastic-brittle bodies with statistically distributed subregions strength values. Frattura Ed Integrita Strutturale, 18(68), pp. 325–339. DOI: 10.3221/IGF-ESIS.68.22.
[17] Wildemann, V.E., Feklistova, E.V., Mugatarov, A.I., Mullahmetov, M.N. and Kuchukov, A.M. (2023). Aspects of numerical simulation of failure of elastic-brittle solids, Comput. Contin. Mech., 16(4), pp. 420–429. DOI: 10.7242/1999-6691/2023.16.4.35.
[18] Ilinykh, A.V. and Vildeman, V.E. (2012). Modeling of structure and failure processes of granular composites, Comput. Contin. Mech., 5(4), pp. 443–451. DOI:10.7242/1999-6691/2012.5.4.52.
[19] Wildemann, V.E. and Ilynykh, A.V. (2007). Simulation of structural failure and scale effects of softening at the post-critical deformation stage in heterogeneous media, Phys. Mesomech., 10(4), pp. 23–29.
[20] Zhou, R., Lu, Y., Wang, L. and Chen, H. (2021). Mesoscale modeling of size effect on the evolution of fracture process zone in concrete, Eng. Fract. Mech., 245, No. 107559. DOI: 10.1016/j.engfracmech.2021.107559.
[21] Lopes, B., Arruda, M.R.T., Almeida-Fernandes, L., Castro, L., Silvestre, N. and Correia, J.R. (2020). Assessment of mesh dependency in the numerical simulation of compact tension tests for orthotropic materials, Compos. Part C Open Access, 1, No. 100006. DOI: 10.1016/j.jcomc.2020.100006.
[22] Hai, L. and Lyu, M.-Z. (2023). Modeling tensile failure of concrete considering multivariate correlated random fields of material parameters, Probabilistic Eng. Mech., 74, No. 103529. DOI: 10.1016/j.probengmech.2023.103529.
[23] Chen, X. and Li, J. (2023). An extended two-scale random field model for stochastic response analysis and its application to RC Short-leg shear wall structure, Probabilistic Eng. Mech., 74, 103508. DOI:10.1016/j.probengmech.2023.103508.
[24] Liu, Y.-Yi, Chen, J.-B. and Li, J. (2024). The modified mesoscopic stochastic fracture model incorporating the random field of Young's modulus for the uniaxial constitutive law of concrete, Probabilistic Eng. Mech., 75, 103585. DOI:10.1016/j.probengmech.2024.103585.
[25] Tretyakova, T.V. and Spaskova, E.M. (2013). Experimental study of the limiting stress-strain states of a quasi-brittle material using the digital image correlation method, PNRPU Mech. Bull., 2, pp. 186–198. DOI:10.15593/perm.mech/2013.2.186-198.